

# Supporting Information

## Endogenous H<sub>2</sub>O<sub>2</sub> self-replenishment and sustainable cascades enhance the efficacy of sonodynamic therapy

Jia-Rui Du, Deng-Ke Teng, Yang Wang, Qimeihui Wang, Yuan-Qiang Lin, Qiang Luo,  
Jia-Nan Xue, Ling-Yu Zhu, Peng Dong, Gen-Mao Zhang, Yan Liu, Zhi-Xia Sun,  
Hui Wang\*, Guo-Qing Sui\*

Department of Ultrasound, China-Japan Union Hospital of Jilin University, No. 126,  
Xian Tai Street, Changchun, 130000 Jilin, China

### Corresponding author:

**Hui Wang**

whui66@jlu.edu.cn

**Guo-Qing Sui**

suiguqing@jlu.edu.cn

These authors contributed equally: Hui Wang and Guo-Qing Sui.

Department of Ultrasound, China-Japan Union Hospital of Jilin University, No. 126,  
Xian Tai Street, Changchun, 130000 Jilin, China

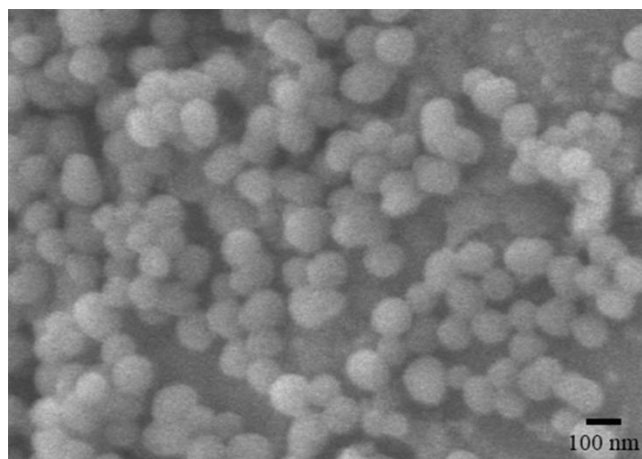


Fig. S1. SEM images of PDA.

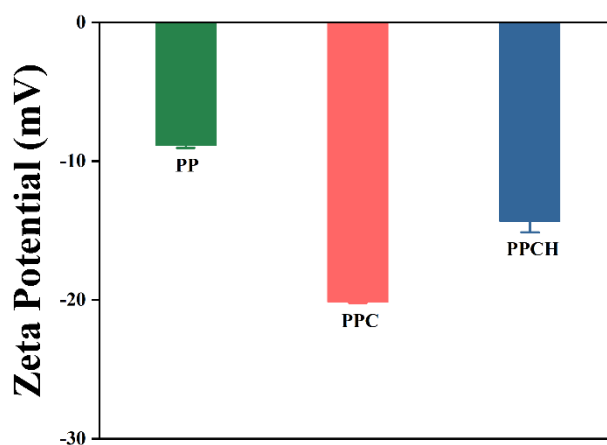


Fig. S2. Zeta-potential values of the PP, PPC and PPCH.

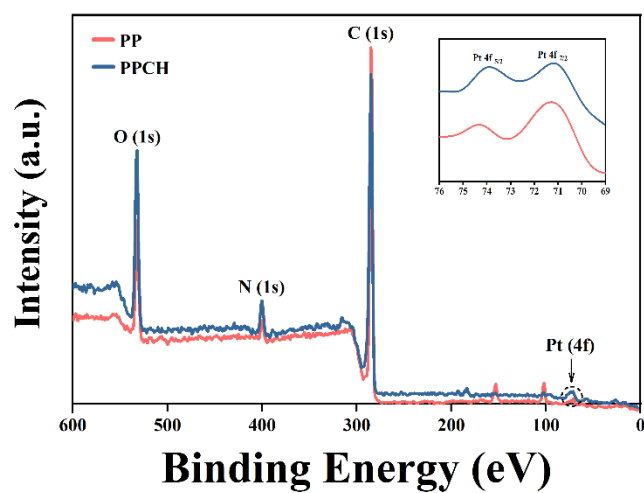


Fig. S3. X-ray photoelectron spectroscopy of PP and PPCH, insert: Pt 4f region.

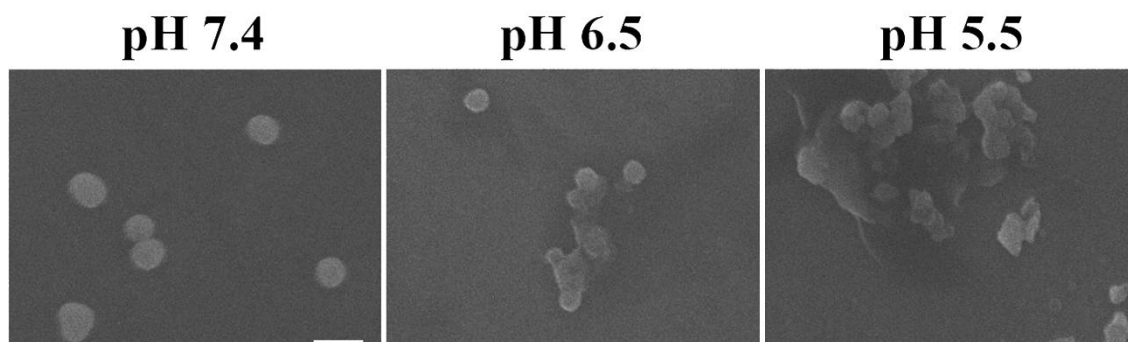


Fig. S4. SEM of the degradation of PPCH at different pH conditions for 5 h  
(Scale bar: 200 nm).

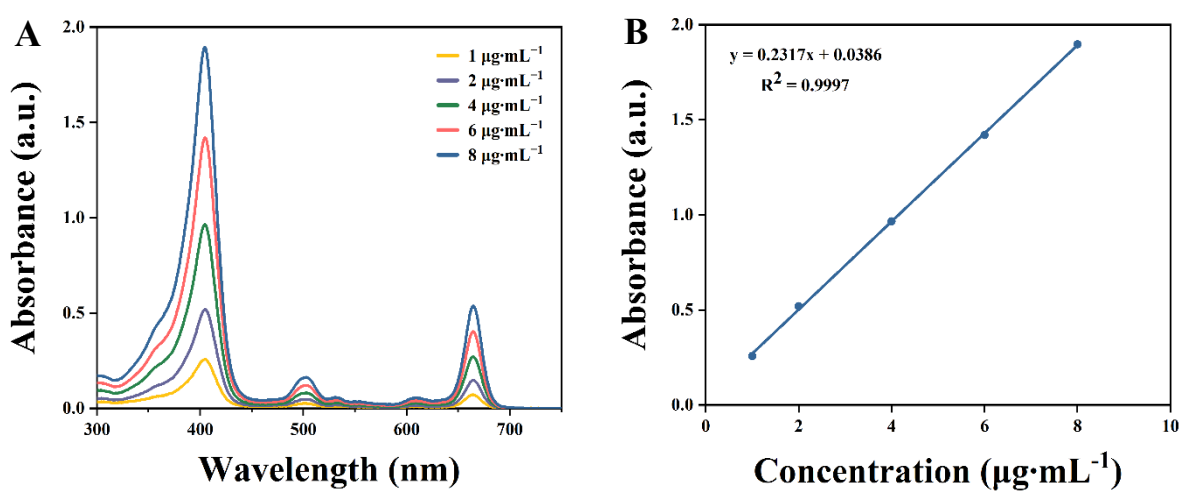


Fig. S5. (A) UV-Vis absorption spectra of different concentrations of Ce6 and  
(B) the fluorescence intensity of different concentrations of nanoplateform.

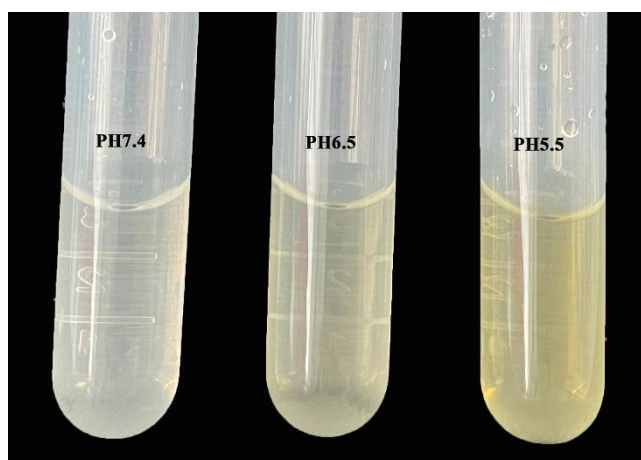


Fig. S6. Photograph of PPCH after immersing in PBS at different pH for 5 h.

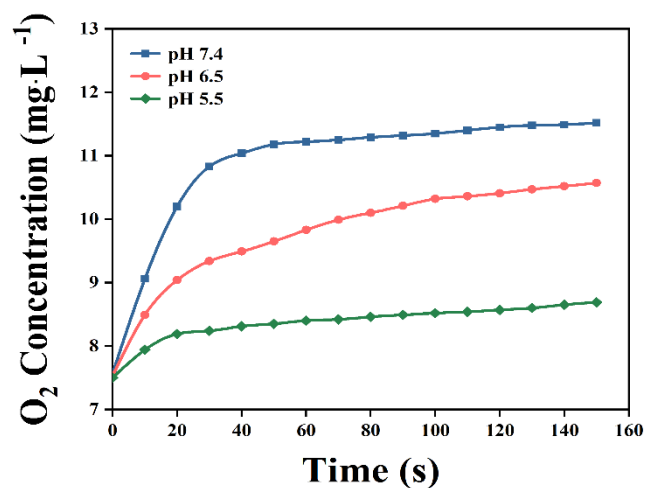


Fig. S7. O<sub>2</sub> generation upon the addition of PPCH and H<sub>2</sub>O<sub>2</sub> in PBS buffer with different pH (5.5, 6.5, and 7.4).

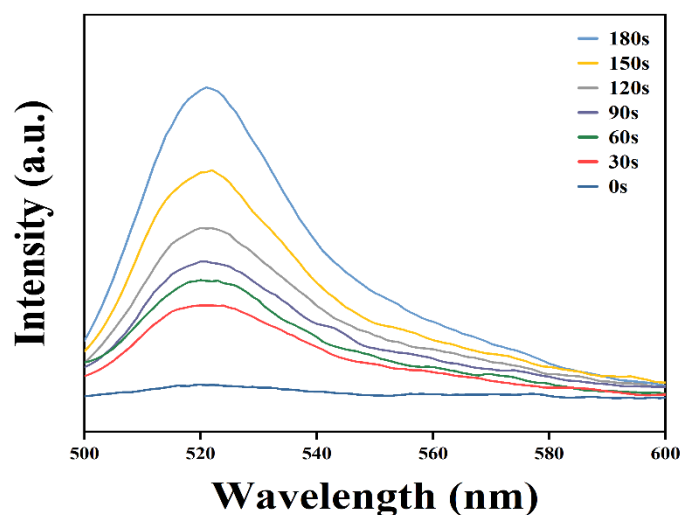


Fig. S8. <sup>1</sup>O<sub>2</sub> production of PPCH irradiated by LIFU during different time.

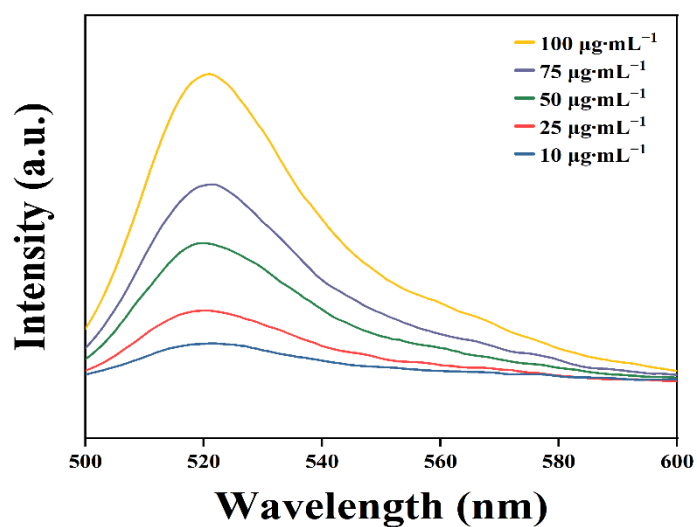


Fig. S9. <sup>1</sup>O<sub>2</sub> generation of PPCH irradiated at different concentration by LIFU.

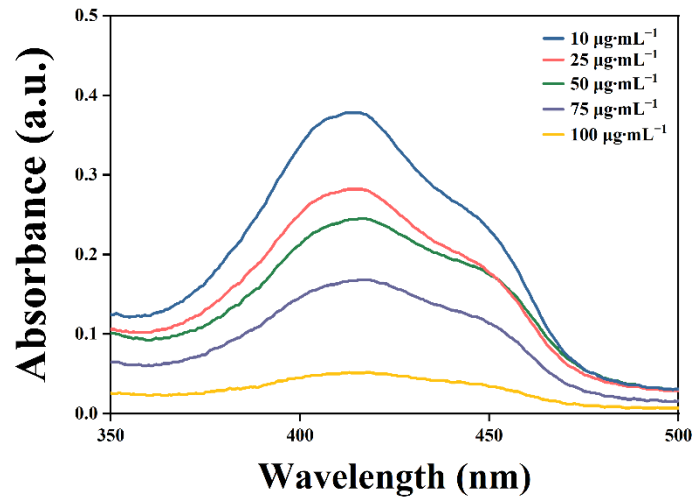


Fig. S10. Uv-Vis absorption spectra of DPBF (410nm) and PPCH solutions with different concentrations under LIFU irradiation.

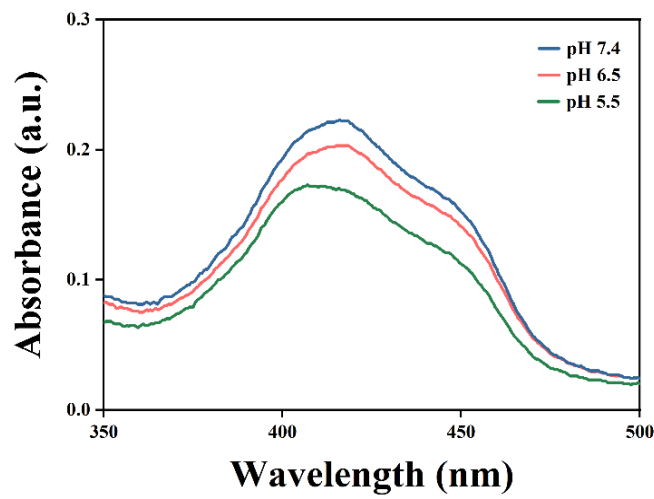


Fig. S11. Uv-Vis absorption spectra of DPBF (410nm) and PPCH solutions at different pH under LIFU irradiation.

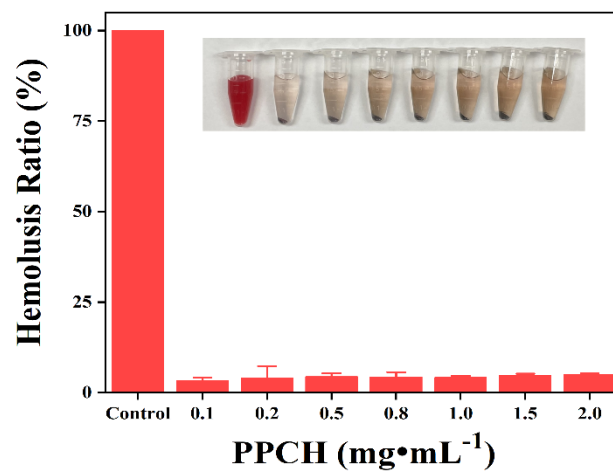


Fig. S12. Hemolysis of PPCH at various concentrations, illustration: 4-hour physical picture of hemolysis experiment.

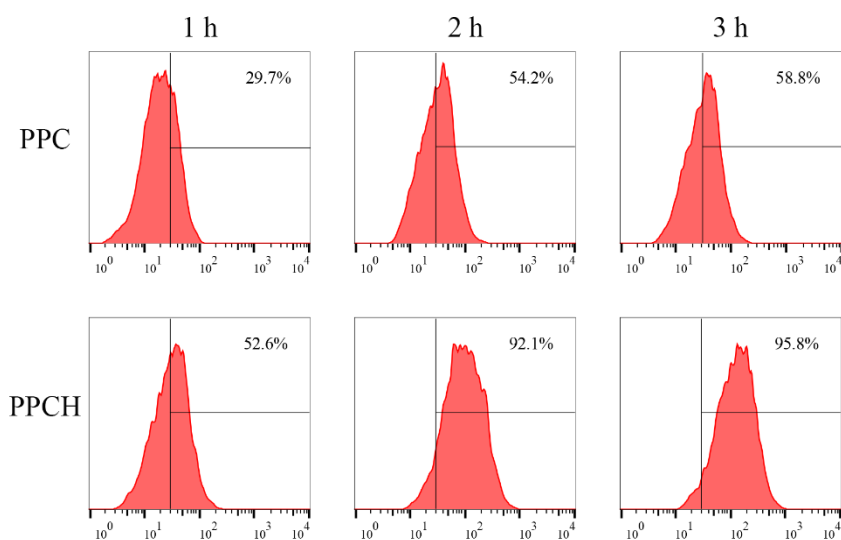


Fig. S13. Quantitative analysis of the cellular uptake behavior of PPCH after different intervals of incubation analyzed by flow cytometry.

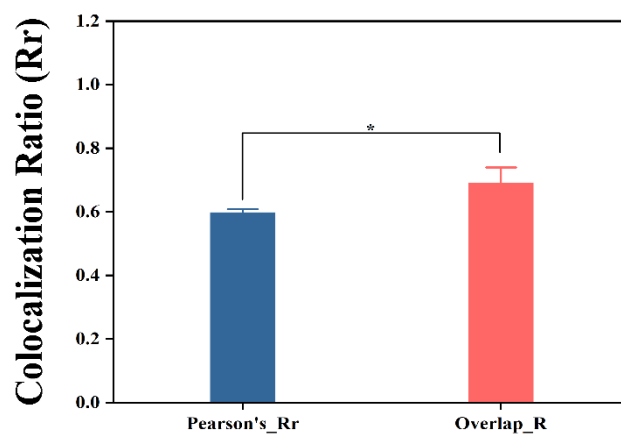


Fig. S14. the statistic of Pearson's correlation coefficient and overlap coefficient (Rr) for Fig 4A.

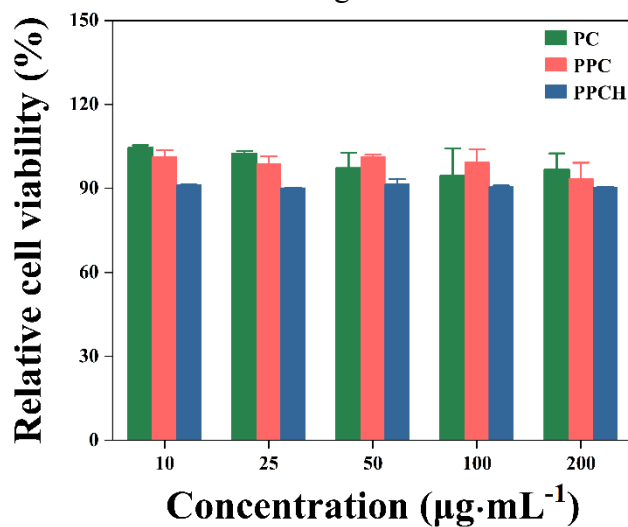


Fig. S15. Relative viability of Huvec cells incubated with PPCH at different concentrations.

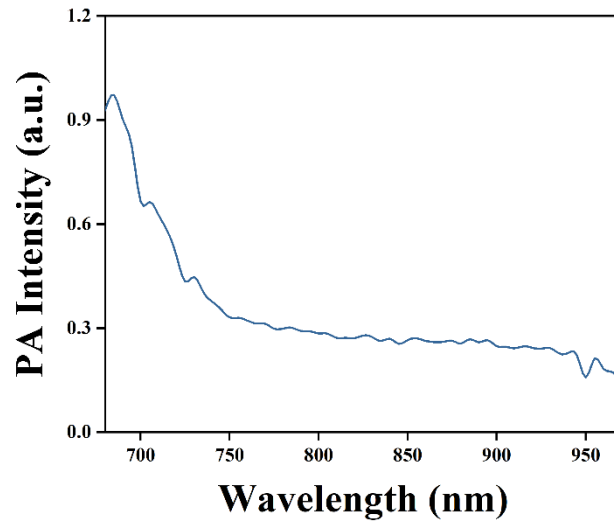


Fig. S16. The peaks of PA intensity of PPCH.

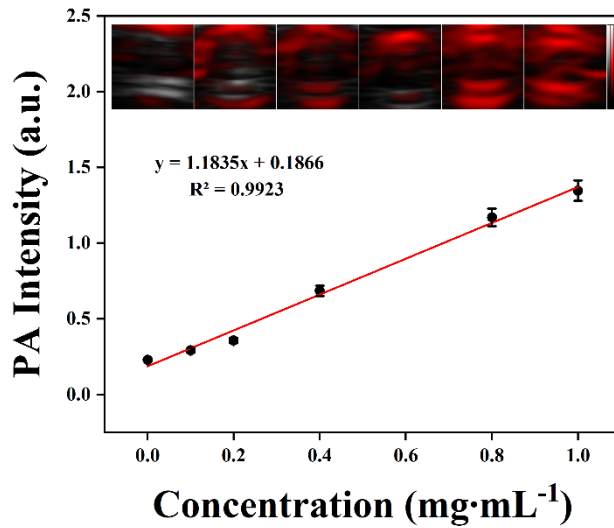


Fig. S17. PA images and their intensities of PPCH in vitro at different concentrations.

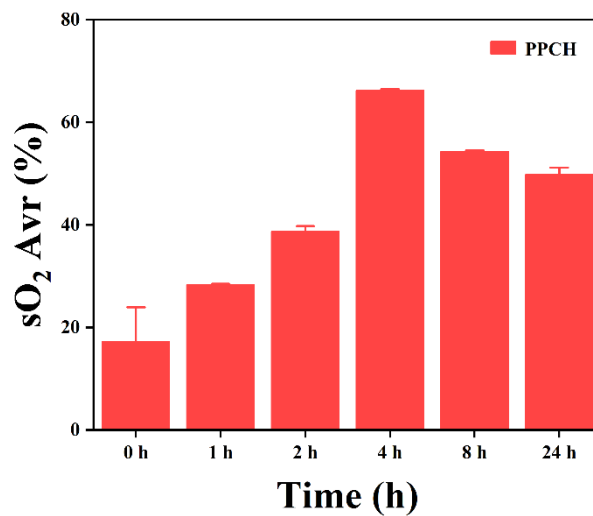


Fig. S18. Quantification of oxyhemoglobin level of tumor in different times.

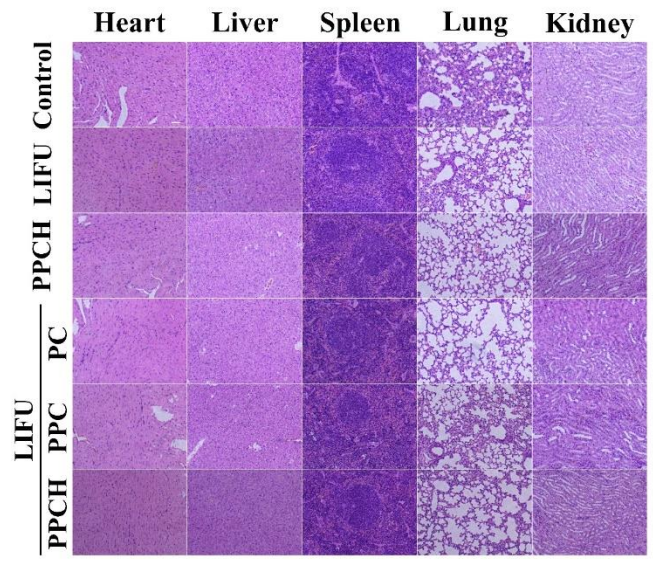


Fig. S19. HE staining of major organs in each group after 18 days of treatment  
(Scale bar: 50  $\mu$ m).